The Journal of Prevention of Alzheimer's Disease 12 (2025) 100087

Contents lists available at ScienceDirect

The Journal of Prevention of Alzheimer's Disease

journal homepage: www.elsevier.com/locate/tjpad

Original Article

LMTK2 and *CRB1* are two novel risk genes for Alzheimer's disease in Han Chinese

Xuewen Xiao[a,b,c,d], Hui Liu[a], Rui Yao[a], Yunni Li[c,d], Xinxin Liao[b,c,d,e], Yingzi Liu[a], Yafang Zhou[b,c,d,e], Junling Wang[a,b,c,d], Beisha Tang[a,b,c,d], Bin Jiao[a,b,c,d], Jinchen Li[b,f], Lu Shen[a,b,c,d], Shilin Luo[a,b,c,d,*]

[a] *Department of Neurology, Xiangya Hospital, Central South University, Changsha, PR China*
[b] *National Clinical Research Center for Geriatric Disorders, Central South University, Changsha, PR China*
[c] *Engineering Research Center of Hunan Province in Cognitive Impairment Disorders, Central South University, Changsha, PR China*
[d] *Hunan International Scientific and Technological Cooperation Base of Neurodegenerative and Neurogenetic Diseases, Changsha, PR China*
[e] *Department of Geriatric Neurology, Xiangya Hospital, Central South University, Changsha, PR China*
[f] *Bioinformatics Center, Xiangya Hospital & Furong Laboratory, Changsha, PR China*

ARTICLE INFO

Keywords:
Alzheimer's disease
Whole-exome sequencing
LMTK2
CRB1

ABSTRACT

Background: Alzheimer's disease (AD) is the most prevalent neurodegenerative disease with a substantial genetic background. However, its underlying genetic architecture remains to be elucidated.
Methods: In this study, we performed whole-exome sequencing in 282 familial and/or early-onset AD patients and 1086 cognitively normal controls in the Han Chinse populations. According to minor allele frequency, variants were divided into common variants (MAF ≥ 0.01) and rare variants (MAF < 0.01). Common variant-based association analysis and gene-based association test aggregating rare variants were performed by PLINK 1.9 and Sequence Kernel Association Test-Optimal, respectively. We replicated the significant results by using the same AD samples and controls from whole genome sequencing (n = 1879). Furthermore, we determined the functions of the novel AD risk genes *in vitro*.
Results: Common variants association analysis revealed that *APOE* rs429358 reached statistical whole-exome significance. Gene-level aggregation testing identified that rare damaging variants in *LMTK2* and *CRB1* conferred risk to AD. All variants are located in highly conserved amino acid regions and are predicted to be damaging. Furthermore, functional studies showed that *LMTK2* rare damaging variants (R234P and S974G) enhanced tau phosphorylation levels, tau aggregates formation, and Aβ generation. Meanwhile, the *CRB1* Y556X variant caused incomplete translation of CRB1 protein and increased the Aβ42 level and Aβ42/Aβ40 ratio.
Conclusion: Our findings indicated that *LMTK2* and *CRB1* are two novel AD risk genes in Han Chinese, which may provide promising targets for diagnosis and intervention.

1. Introduction

Alzheimer's disease (AD) is the most prevalent neurodegenerative disease and one of the most burdening diseases worldwide [1]. AD is characterized by progressive cognitive impairment and a decline in personal daily activities. The typical neuropathologic hallmarks include extracellular β-amyloid (Aβ) plaque accumulation and intracellular neurofibrillary tangles of hyperphosphorylated Tau [2]. Genetic, environmental, and aging factors contribute to AD, among which genetic factors play a strong role. According to age at onset (AAO), AD is classified into early-onset AD (EOAD, typically AAO < 65 years) and late-onset AD (LOAD, typically AAO ≥ 65 years). LOAD is a complex disease with a heritability of 58–79 %, while EOAD is almost entirely genetically determined, and heritability ranges from 92 % to 100 % [3]. Using linkage analyses, three causal genes of AD were identified, namely *APP* (Aβ precursor protein), *PSEN1* (Presenilin-1), and *PSEN2* (Presenilin-2) genes [4–6]. Our group previously identified that only 1.65 % of EOAD patients carried disease-causing variants in the *APP, PSEN1*, and *PSEN2* genes in the Han Chinese population [7]. In the Caucasian population, roughly 1.35 % of EOAD patients carried the disease-causing gene variants in these genes [8]. These studies suggest that the proportion of causal gene variants in AD is relatively low, and there are still other causal and/or susceptibility genes to be explored.

* Corresponding author at: Department of Neurology, Xiangya Hospital, Central South University, 87 Xiangya Rd, Changsha, PR China.
E-mail address: Shilin_luo@csu.edu.cn (S. Luo).

https://doi.org/10.1016/j.tjpad.2025.100087
Received 27 December 2024; Received in revised form 30 January 2025; Accepted 2 February 2025
Available online 7 February 2025

Genome-wide association studies (GWASs) identified more than eighty AD/dementia susceptibility loci. Nevertheless, most loci are located in non-coding regions with small to moderate effect sizes and capture a fraction of the heritability, and almost 59 % of AD heritability remains unexplained. The missing heritability can be attributed to many factors, including rare variants [9]. Thanks to the advances of next-generation sequencing technologies, dozens of rare variants with larger effect sizes were identified in AD, such as *UNC5C* [10], *TREM2* [11], and *PLD3* [12]. However, most genetic studies are from Caucasian populations, and population heterogeneity exists towards genetic risk factors. For example, even the most important risk gene, *APOE*, its risk level varies among different populations. The risk of *APOE* $\varepsilon 4$ decreased following East Asian, White, Black, and Hispanic [13]. Thus, given that the number of AD patients in China accounts for about 25 % of dementia patients worldwide [14], it is important to investigate the genetic factors in the Chinese population. In this study, we conducted whole-exome sequencing (WES) of AD patients and health controls, and identified two novel susceptibility genes, *LMTK2* and *CRB1*, in the Chinese population, as well as confirmed the variants in *LMTK2* and *CRB1* could induce the onset of AD in the *in vitro* experiments.

2. Materials and methods

2.1. Subjects

To increase the possibility of identifying true AD risk genes, an extreme phenotype sampling strategy was applied in the WES stage according to a previous report [15]. The inclusion criteria of AD patients include (i) AAO ≤ 55 years old and/or (ii) with a positive family history. 282 AD patients met the criteria from Xiangya Hospital and 1086 health controls from a community in Hunan, China. All of them were from Central Southern China, including the provinces of Hunan, Jiangxi, Hubei, and Guizhou. We only included the probands for familial AD patients, and no other family members were enrolled. The AD patients were diagnosed by two neurologists using the National Institute on Aging-Alzheimer's Association criteria for probable AD [16]. Participants with causative variants for AD (*APP, PSEN1*, and *PSEN2*) had been excluded using Sanger sequencing. Several neuropsychological tests were conducted on the AD patients by an experienced clinical neuropsychologist, including the Mini-Mental State Exam (MMSE), Montreal Cognitive Assessment (MoCA), the activity of daily living (ADL), and Neuropsychiatric Inventory (NPI), and Clinical Dementia Rating (CDR). The health controls showed no cognitive impairment using clinical inquiries and MMSE assessments. This study was approved by the Institutional Review Board of Xiangya Hospital, Central South University. Written informed consent was obtained from each participant or their guardian.

2.2. Whole-exome sequencing and whole-genome sequencing

Genomic DNA was extracted from peripheral blood leukocytes. All DNA samples were normalized to 100 ng/μL. The SureSelect Human All Exon Kit V6 (Agilent) captured whole-exome DNA on the Illumina × 10 platform. The average depth was 129 ×, and the percentage of base sequences ≥10 × reached more than 99 %. Whole-genome sequencing (WGS) was performed on each participant on the BGI-seq 500 platform (BGI, Shenzhen, China). The mean WGS depth was 30 × per sample on average in our cohort. The low-quality reads of fastq data were removed by FastQC (http://www.bioinformatics.babraham.ac.uk/projects/fastqc/).
Then, paired-end sequence reads were aligned to the human reference genome (UCSC hg19) using the Burrow-Wheeler Aligner software (http://bio-bwa.sourceforge.net) [17]. Picard (http://broadinstitute.github.io/picard/) was used to remove duplicate sequence reads, generate the converse format, and index the sequencing data. The base quality-score recalibration, local realignments around possible insertions/deletions (indels), variant calling, and filtering were conducted with the Genome Analysis Toolkit (https://software.broadinstitute.org/gatk/) [18]. The variants were annotated using ANNOVAR (https://hpc.nih.gov/apps/ANNOVAR.html) [19] and VarCards (http://genemed.tech/varcards/) [20], such as regions, amino acid alterations, and allele frequencies. Variants were classified into common variants and rare variants based on minor allele frequencies (MAF) at a threshold of 0.01 (common variants: MAF ≥ 0.01; rare variants: MAF < 0.01). In our study, ReVe, an algorithm developed by our group, and CADD were used to predict deleterious missense variants. The damaging variants were defined by loss-of-function (LoF) or missense variants with ReVe ≥ 0.5 [20] and CADD ≥ 20 [21]. LoF variants involved variants resulting in stop, frameshift, or splice-site disruption. The variants were named according to the Human Genome Variation Society guidelines [22]. Sanger sequencing was carried out in patients with significant genes.

2.3. Quality control

The VCF data were recoded into PLINK format for variant and individual quality control using PLINK v1.9 [23]. We filtered out variants with genotyping rate < 95 %, Hardy–Weinberg equilibrium P value < 1×10^{-6} in the controls, genotype quality ≤ 30, depth ≤ 20, allelic balance out of 25 %/75 % ratio of referent and alternate allele reads in the heterozygote, and allelic balance out of 95 % ratio in the homozygote. Individuals were excluded if they had conflicting sex assessments between recorded sex and inferred sex, cryptic relatedness (identity by descent > 0.125), too much missing genotype data (> 5 % missing genotypes), and deviating heterozygosity (±3 standard deviations). The principal component analysis (PCA) was conducted on the remaining participants to remove the outliers.

2.4. Antibodies

The following primary antibodies were used: anti-Flag (Proteintech, #66008–4-lg), anti-Tau5 (Invitrogen, #13–6400), anti-p-Tau T181 (Invitrogen, #701530), anti-p-Tau S202 (Abcam, #ab108387), anti-p-Tau S396 (Invitrogen, #44–752 G), anti-p-PP1α (Cell signaling Technology, #2581), anti-PP1C (Abcam, #AB134947), anti-p-GSK3β Ser9 (Cell signaling Technology, #5558), anti-BAX (Proteintech, #50599-2-lg), anti-Bcl2 (Proteintech, #12789-1-AP), anti-GAPDH (Proteintech, #60004-1-lg), anti-GSK3β (Cell Signaling Technology, #12456), anti-Flag (Proteintech, #20543-1-AP), anti-APP (Abcam, #32136), anti-ADAM10 (Cell Signaling Technology, #14194), anti-BACE1 (Abcam, #ab108394), anti-PSEN1 (Proteintech, 16163-1-AP), anti-PSEN2 (Proteintech, 116168-1-AP), and anti-β-tubulin (Proteintech, #10,094–1-AP).

2.5. Cell lines and transfection

HEK293, HEK293-APPswe, and HEK293-Tau RD (repeat domain) cells were cultured in high-glucose DMEM and SH-SY5Y-APPswe cells in high-glucose DMEM/F12. The cultural medium was supplemented with 10 % FBS and penicillin (100 units/mL)/streptomycin (100 μg/mL). All high-expression plasmids were constructed by Genscript Biotech (Nanjing, China) with pcDNA 3.1 backbone. The cell transfection was performed using Lipofectamine 3000 (Invitrogen, #L3000075) according to the manufacturer's protocol with Opti-MEM (Invitrogen, #31,985,070) as the transfection solution. Transfected cells were incubated at 37 °C for 48 h and harvested for further experiments.

2.6. Transduction of cells with PFFs

Tau-RD domain (K18, 1 mg/mL) was transduced into HEK293-Tau RD cells according to the previously described method [24]. Briefly, after the plasmid transfection for 24 h, one microgram of K18 was combined with Opti-MEM and then added to another tube with 96 μL of

Opti-MEM and 4 μL of Lipofectamine 3000. The reagents were incubated for 20 min and then added to the culture medium. To observe Tau aggregates, cells were fixed with 4 % paraformaldehyde for 10 min at room temperature, followed by DAPI staining for 5 min. The cell sections were mounted to take pictures on a microscope (Leica Thunder).

2.7. Western blotting

To prepare whole-cell lysates, the mouse brain tissues were lysed in RIRA buffer (NCM, #WB3100) containing a mixture of protease and phosphatase inhibitors on ice for 15 min. Lysates were centrifuged at 15,000 rpm for 15 min at 4 ˚C, and then the supernatant was collected and subjected to protein concentration determination by BCA assay. An equal amount of protein was loaded for immunoblotting with specific antibodies indicated.

2.8. Aβ42/Aβ40 quantification

The quantification of Aβ40 and Aβ42 was measured using an enzyme-linked immunosorbent assay (ELISA). The SH-SY5Y-APPswe cells culture medium was collected from each test group and centrifuged. The supernatants were collected, and the levels of Aβ40 and Aβ42 were determined in accordance with the operating instructions of the human Aβ40 ELISA kit (Elabscience, #E-EL-H0542) and human Aβ42 ELISA kit (Elabscience, #E-EL-H0543), respectively.

2.9. Statistical analysis

For common variants, logistic regression analysis was performed to test the allele dosage difference between AD patients and controls. For rare variants, using the Sequence Kernel Association Test-Optimal (SKAT-O test) [25], the gene-based association tests were performed by aggregating rare variants with a MAF threshold of ≤ 1 % and a minor allele count ≥2 between AD patients and controls [26]. Rare variants were classified into several groups: rare damaging variants, rare damaging missense variants, rare LoF variants, and rare missense variants. Age, sex, *APOE* ε4 status (*APOE* ε4+, *APOE* ε4–), and the first five principal components were adjusted in the common and rare variant association analyses. A cutoff P value * $n < 0.05$ was statistically significant (n is defined by the number of variants or genes). All experimental data were expressed as mean ± SEM from three or more independent experiments. Histological data were analyzed using either Student's t-test (two-group comparison) or one-way ANOVA with Tukey's multiple-comparisons test. The threshold for significance for all experiments was set $^{*}P < 0.05$, and smaller P values are represented as $^{**}P < 0.01$ and $^{***}P < 0.001$.

3. Results

3.1. Demographic and clinical information

We applied an extreme phenotype sampling strategy to perform WES to increase the likelihood of identifying the true risk variants. A total of 282 unrelated AD patients with an early AAO (AAO ≤ 55) and/or family history. Among them, there are 168 participants with AAO ≤ 55 years old, 40 of whom have a positive familial history. Also, 1086 normal controls were enrolled. The average AAO of AD patients was 59.70 years, and the average age of controls was 68.00 years. There was a significant difference between AD patients and controls concerning age ($P < 0.001$). The MMSE scores of AD patients were significantly lower than those of controls ($P < 0.001$), and the average MoCA, CDR, ADL, and NPI scores were 7.52, 1.27, 32.05, and 16.80, respectively (Supplementary Table 1). Meanwhile, we enrolled 1879 controls for replication using WGS. The average enrolled age was 65 years old, which was also lower than the AAO of the AD patients ($P < 0.001$). Similarly, the mean MMSE score was 26 and higher than that of the AD group ($P < 0.001$). The controls of WGS did not overlap with those of WES.

3.2. Common variant association test

After sample quality control, 5 AD patients and 45 controls were excluded. Thus, a total of 277 AD patients and 1041 controls were included in subsequent association analysis. For common variants, after variation quality control, a total of 121,333 common variants were included in the analysis. The plot of PCA indicated that the population structure of AD and control group was consistent (Supplementary Fig. 1A), and the genomic inflation factor was 0.957. The QQ plot showed no obvious stratification in the population (Supplementary Fig. 1B). After adjusting for confounding factors, including sex, age, *APOE* ε4 carrier status (*APOE* ε4 + and *APOE* ε4 −), and principal components, only *APOE* rs429358 reached the level of statistical difference across the exome ($P = 4\ 0.10 \times 10^{-7}$) (Supplementary Fig. 1C).

3.3. Gene-level aggregation testing identified LMTK2 and CRB1 as novel AD risk genes

After quality control, rare variants were collapsed together and the SKAT-O test analyzed their joint effects. When analyzing the rare damaging missense variants, 10,627 genes were left, and we identified that *LMTK2* reached statistical significance between AD patients and controls (adjusted $P = 3.37 \times 10^{-6}$) (Fig. 1A). Specifically, two rare damaging missense variants, p.R234P and p.S974G existed in two and three AD patients, respectively. However, these variants were absent in controls (Fig. 1B). Furthermore, in the rare damaging variant group, 7317 genes were included for analysis. Among them, *CRB1* is significantly associated with AD (adjusted $P = 5.33 \times 10^{-8}$) (Fig. 2A). A total of four rare damaging variants were found in the *CRB1* gene. Among them, p.E153 K was identified in 14 AD patients and 9 controls. Both p.Y655X and p.C1124R were detected in two AD patients and absent in controls. Moreover, one AD patient and one control carried p.A1304D in the *CRB1* gene (Table 1) (Fig. 2B). *LMTK2* and *CRB1* rare variants were confirmed by Sanger sequencing. All of the abovementioned variants are located in highly conserved amino acid regions (Figs. 1C and 2C), among which the missense variants are classified as damaging by ReVe and CADD. Using a public brain single-nuclei RNA sequencing (RNA-seq) study from AD patients and controls, we found that LMTK2 and CRB1 are expressed in almost all kinds of cells, including neurons and neurogliocytes (Supplementary Fig. 2).

3.4. Replication of the association of LMTK2 and CRB1 with AD

To verify the association of *LMTK2* and *CRB1* with early-onset and familial AD, we screened these variants using the same AD patients from WES ($n = 282$) and controls from WGS ($n = 1879$). We successfully replicated the association of *LMTK2* and *CRB1* rare variants with AD. Specifically, rare variants of *LMTK2* (adjusted $P = 1.88 \times 10^{-6}$) and *CRB1* (adjusted $P = 1.54 \times 10^{-5}$) conferred risk to AD in the replication stage. In the combined analysis with all samples, including 282 CE patients and 1082 controls in the WES stage, as well as 1879 controls from the WGS stage, which demonstrated that both *LMTK2* (adjusted $P = 3.52 \times 10^{-9}$) and *CRB1* (adjusted $P = 5.83 \times 10^{-7}$) rare variants were associated with AD risk (Table 1). Additionally, we successfully replicated the *LMTK2* and *CRB1* rare damaging variants by using the same AD patients and replacing controls from gnomAD and ChinaMAP ($P < 0.05$) (Supplementary Table 2).

3.5. LMTK2 rare variants augment tau phosphorylation and Aβ generation

To investigate the effects of *LMTK2* rare variants on tau phosphorylation, Different Flag-LMTK2 plasmids (vector, WT, R234P, and S974G) were co-transfected with equal human HA-Tau into HEK293 cells. Immunoblotting showed that overexpression of LMTK2 WT significantly reduced p-Tau T181, S202, and S396 levels compared to that in the vector group. However, compared to the WT group, the levels of these

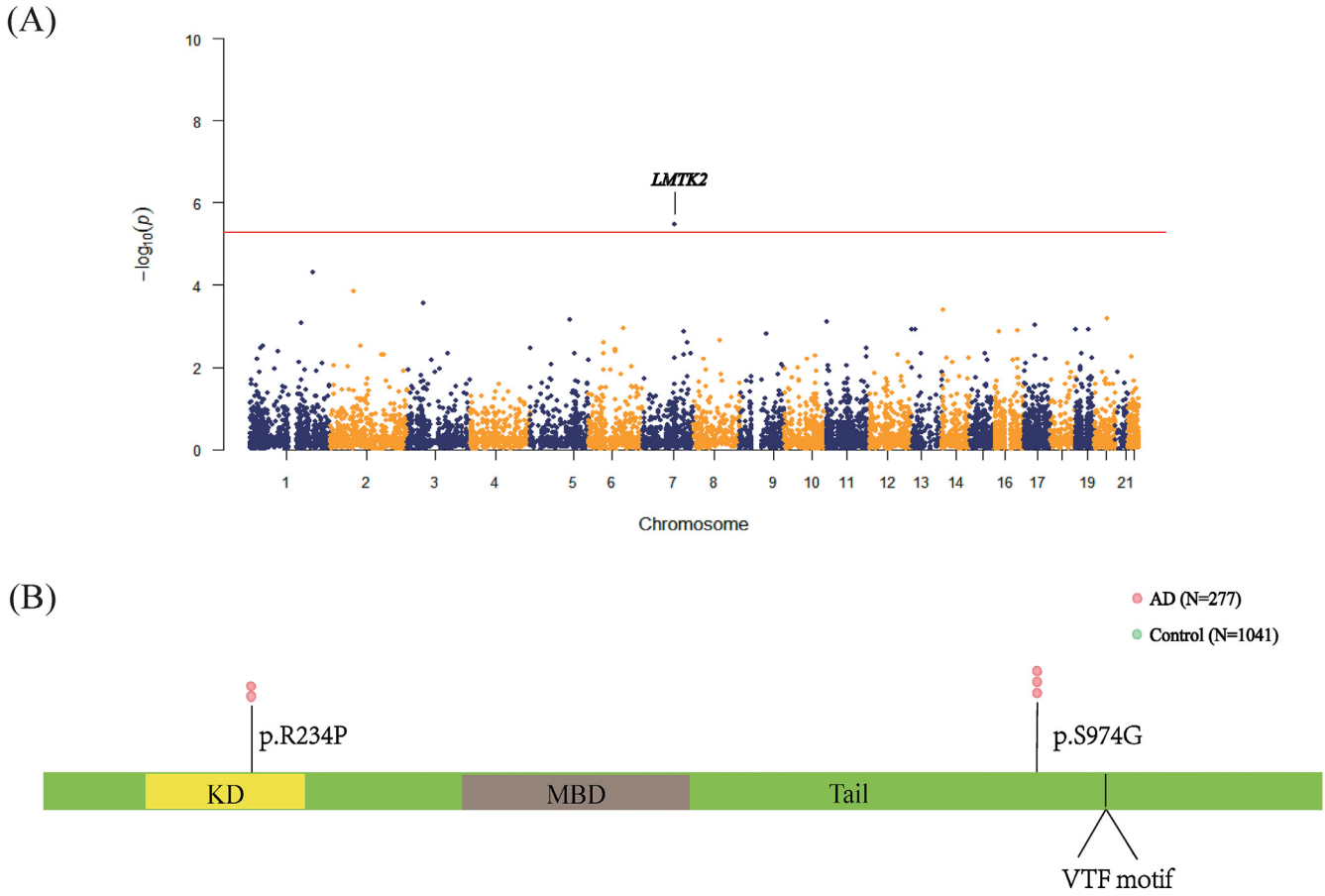

Fig. 1. *LMTK2* rare damaging variants with early-onset and/or familial AD. (A) Manhattan plot of the exome-wide rare damaging missense variants association analysis Red line indicates the exome-wide significance (10,627 genes were included, P value $< 4.70 \times 10^{-6}$ (0.05/10,627) was significant). (B) Rare damaging missense variants in the *LMTK2* gene in AD patients and controls. LMTK2 contains a kinase domain (KD), a Myosin VI binding domain (MBD), and a tail domain. (C) The p.R234P and p.S974G are conserved in different species, which are highlighted in the red boxes.

Table 1
LMTK2 and *CRB1* rare variants conferred risk for AD in Han Chinese.

Gene	Variant	AD	Control		ReVe	CADD	Adjusted P		
			WES	WGS			WES	WGS	combined
LMTK2	c.701G>C:p.R234P	2/554	0/2082	0/3758	0.568	20.6	3.37×10^{-6}	1.88×10^{-6}	3.52×10^{-9}
	c.2920A>G:p.S974G	3/554	0/2082	4/3758	0.749	26.3			
CRB1	c.457G>A:p.E153K	14/554	9/2082	27/3758	0.714	25.3	5.33×10^{-8}	1.54×10^{-5}	5.83×10^{-7}
	c.1965T>A:p.Y655X	2/554	0/2082	0/3758	–	33			
	c.3370T>C:p.C1124R	2/554	0/2082	0/3758	0.935	26			
	c.3911C>A:p.A1304D	1/554	1/2082	0/3758	0.746	24.1			

Abbreviations: Adjusted P: adjusted by age, sex, *APOE* ε4 carrier status, and PC1-PC5.

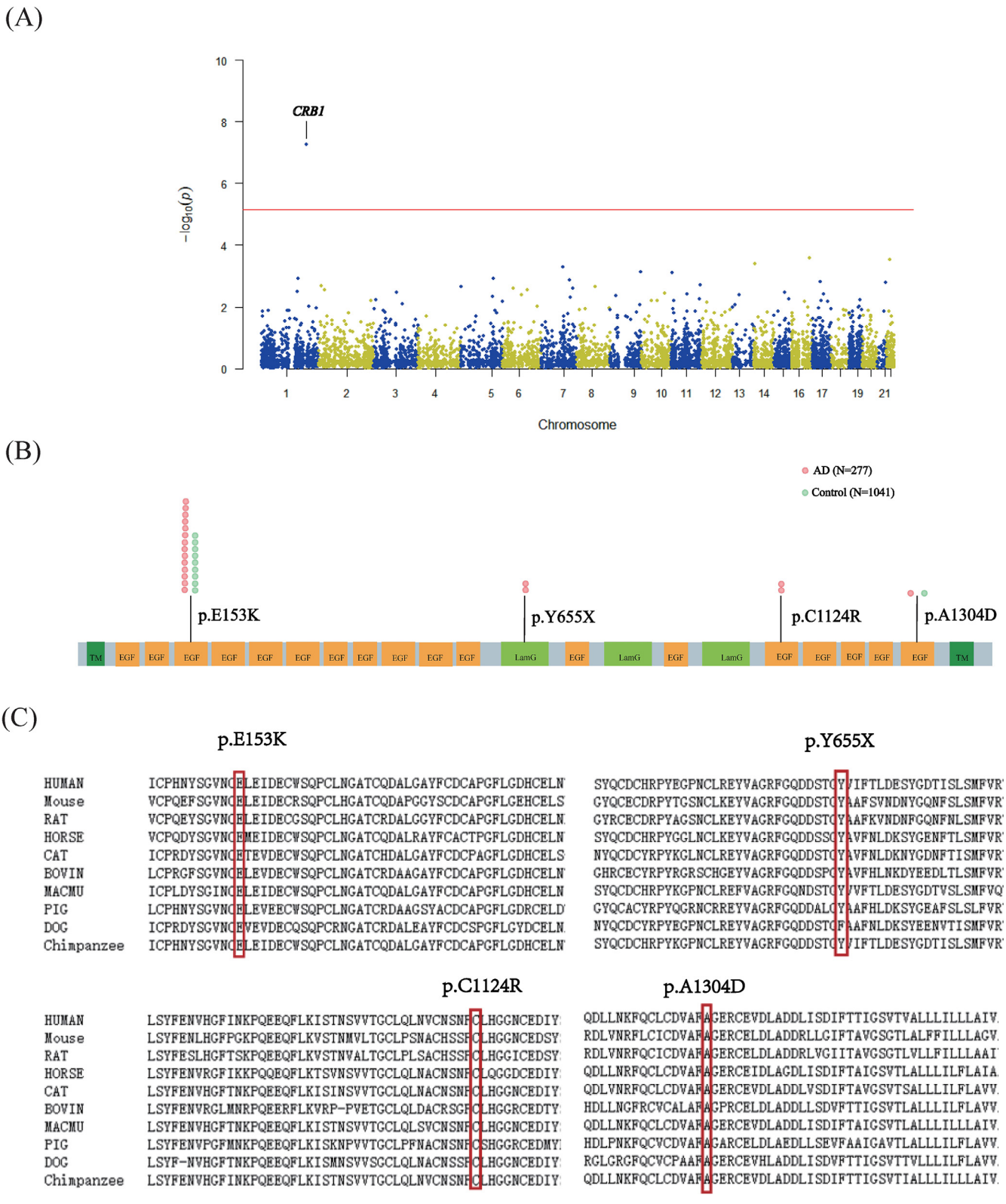

Fig. 2. *CRB1* rare damaging variants with early-onset and/or familial AD. (A) Manhattan plot of the exome-wide rare damaging variants association analysis. The red line indicated the exome-wide significance (7317 genes were included, *P* value < 6.83×10^{-6} (0.05/7317) was significant). (B) Rare damaging variants in the *CRB1* gene in AD patients and controls. CRB1 contains transmembrane (TM) domains, epidermal growth factor-like (EGF) domains, and Laminin G (LamG) domains. (C) The p.E153 K, p.Y655X, p.C1124R, and p.A1304D in the *CRB1* gene are conserved in different species. The variants are highlighted in the red boxes.

tau phosphorylation sites were significantly augmented in response to the LMTK2-R234P and S974G mutant proteins (Fig. 3A and B). As reported in a previous study [27], transduction of Tau PFFs induces the formation of Tau aggregation in the HEK293-Tau RD cells. We further compared the seeding activity of PFFs formed by K18 in the presence of LMTK2 WT and variants (R234P and S974G). Microscopic observation demonstrated that K18-induced Tau aggregates formation and LMTK2 WT significantly blocked the process, but the aggregates significantly augmented in the presence of R234P or S974G variant in LMTK2 compared to the WT group (Fig. 3C and D). To further explore the possible mechanism of increased Tau phosphorylation caused by *LMTK2* variants, we detected the activity of PP1C and GSK3β because the LMTK2/PP1C/GSK3β signaling pathway plays a crucial role in neuronal outgrowth and development and axonal transport [28]. As expected, activated LMTK2 inactivated PP1C by phosphorylating it, which leads to increased phosphorylation of GSK3β. However, there was a significant loss of this regulatory function of LMTK2 caused by the R234P or S974G variant (Fig. 3E and F), which led to Tau aggregation.

Additionally, to investigate the effects of the *LMTK2* rare variants on Aβ and cell apoptosis, LMTK2 WT and its variants were transfected into SH-SHY5Y-APPSwe cells. ELISA demonstrated that WT significantly reduced the levels of Aβ42 and Aβ40 compared to the vector group, and R234P and S974G variants weakened this effect even though the ratio of Aβ42/Aβ40 did not significantly change (Fig. 3G). Meanwhile, immunoblotting showed that the levels of apoptotic proteins BAX (BCL2 associated X) and BCL2 in SH-SHY5Y-APPSwe cells have no significant alteration among LMTK2 groups (Fig. 3H and I). Thus, these results confirm that both LMTK2 variants in R234P or S974G could induce Tau aggregations and Aβ generation *in vitro*.

3.6. CRB1 Y556X variant increased amyloidogenesis

Human CRB2 inhibits γ-secretase cleavage of APP by incorporating itself into the γ-secretase complex [29]. To investigate the effect of *CRB1* rare variants on APP processing and Aβ generation, we transfected CRB1 WT and variants plasmids (E153 K, Y655X, C1124R, and A1304D) into SH-SY5Y-APPSwe cells. Y665X variant resulted in the incomplete translation of CRB1 protein and markedly reduced the APP level compared to other groups (Fig. 4A and B). The expression of other secretases involved in APP cleavages, such as ADAM10, BACE1, PSEN1, and PSEN2, has no significant alterations between WT and variants (Fig. 4A). Furthermore, secreted Aβ42 and Aβ40 in a conditioned medium from these cells were quantified by ELISA. In alignment with APP expression, Y655X markedly increased the Aβ42 levels compared to CRB1-WT, though no significant alteration was observed in Aβ40 (Fig. 4C and D). The Aβ42/Aβ40 ratio considerably increased following CRB1 Y655X transfection, while the other CRB1 variants did not exhibit notable changes relative to WT, at least for amyloidogenesis.

4. Discussion

To date, the vast majority of AD genetic studies were conducted in the Caucasian population. Nevertheless, although China likely has the largest number of AD patients globally, only a few genetic studies focused on the Chinese population [30]. Given the increased burden of AD and racial differences, it is essential to investigate the genetic architecture of AD in the Chinese population. Compared to LOAD or sporadic AD patients, EOAD or FAD patients have a higher heritability and it more likely to identify causal or risk AD genes. For example, in 107 EOAD (AAO $\leq$ 55) and/or FAD patients and 368 controls in the Chinese population, a rare missense variant in the *C7* gene conferred a risk of AD [15]. To increase the likelihood of identification of AD-associated genes, we performed WES in AD patients (extremely early onset/familial) and normal controls using an extreme phenotype sampling strategy. In the present study, we reported that rare variants in *LMTK2* and *CRB1* as two novel genes increased the risk of AD in the Chinese population.

LMTK2 gene is located at 7q21.3 and consists of 14 exons, and its encoded protein is a member of the membrane-anchored serine/threonine-specific protein kinase family [31]. As a brain-enriched kinase regulating fundamental cellular pathways, LMTK2 was reported to be implicated in neurodegenerative diseases through functional experiments. LMKT2 is predominantly expressed in the brain, most notably in the hippocampus and cerebral cortex [32]. Neuropathological studies revealed that LMTK2 levels were decreased in the post-mortem AD cortex compared to age-matched normal controls [33,34]. Several cellular mechanisms underlying LMTK2 may contribute to AD pathogenesis, including tau hyperphosphorylation, impaired axonal transport, apoptosis, ferroptosis, and oxidant damage [28,35]. Our study firstly indicated that rare damaging missense variants in the *LMTK2* gene are associated with AD risk genetically. Intracellular accumulation of hyperphosphorylated tau as neurofibrillary tangles (NFT) is one of the most prominent characteristic hallmarks of AD [36]. CDK5 and GSK3β are two major tau kinases implicated in tau hyperphosphorylation *in vivo*. Under normal conditions, the LMTK2-mediated pathway enables CDK5 to phosphorylate protein phosphatase-1C (PP1C) at threonine-320, hence enhancing the inhibitory phosphorylation of GSK3β at serine-9, which leads to reduced GSK3β activity [37,38]. Consequently, in AD, it was supposed that reduced LMTK2 causes the overactivation of GSK3β and ultimately increases the level of tau phosphorylation [33]. In postmortem AD samples, LMTK2 level was negatively correlated with phospho-tau and NFT pathology [39]. Also, in the cortex of transgenic Tau P301L mice, LMTK2 was reduced using a genome-wide gene expression analysis [40]. In the cell model, we first identified that wild LMTK2 diminishes the phosphorylation level of tau protein, further indicating that LMTK2 can inhibit tau phosphorylation. Moreover, after the overexpression of R234P and S974G mutant LTMK2 protein, the inhibitory effect was weakened. Thus, *LMTK2* rare damaging variants may exert an effect on AD pathogenesis by elevating tau phosphorylation.

Intriguingly, for the first time, our studies revealed that overexpression of wild-type LMTK2 reduced Aβ42 and Aβ40 levels. Meanwhile, compared to wild-type LMTK2 protein, over-expression of R234P and S974G mutant LMTK2 proteins led to elevated Aβ42 and Aβ40 levels. The "amyloid hypothesis" is a widely influential hypothesis, which holds that Aβ accumulates to form oligomers in the brain, and then deposits to form plaques, causing neuronal degeneration and cognitive impairment [41]. APP is cleaved by the β-secretase (BACE1) enzyme initially and processed by the γ-secretase complex which results in the production of Aβ. Over-activation of GSK3β enhances BACE1 enzymatic cleavage of APP and PSEN1 activity, resulting in elevated levels of Aβ42 and Aβ40 [42]. Therefore, it is conceivable that LMTK2 may diminish GSK3β activity, leading to reduced Aβ levels. In fact, in addition to LMTK2, several AD well-established genes are not only associated with the overproduction of Aβ but also participate in tau phosphorylation, such as *BIN1* and *PICALM* [43–45]. In this study, we observed that LMTK2 influenced tau phosphorylation and linked with the levels of Aβ42 and Aβ40, indicating that rare harmful variations of *LMTK2* contribute to the etiology of Alzheimer's disease by impacting tau and Aβ metabolism.

Additionally, we discovered that the rare harmful variants of *CRB1* were prevalent in AD patients, comprising three rare damaging missense variants and one stop-gain variation (Y655X). *CRB1* is located at lq31.3 and encodes a member of the Crumbs protein homologues, featuring many epidermal growth factor-like and laminin A globular-like domain, which plays a crucial role in retinal development and integrity [46]. Variants in the *CRB1* gene are linked to a wide range of retinal dystrophies that result in significant vision impairment [47]. In addition to the eye, CRB1 is expressed in the cerebellum, hippocampus dentate gyrus, olfactory bulbs, rostral migratory stream, and the subventricular zone next to the telencephalic ventricles in the adult mouse brain [48]. Notably, the human protein atlas indicates that CRB1 is expressed in various brain areas, including the cerebral cortex, amygdala, and hippocampus [49]. In the cortex of CRB1rd^8 mutant mouse brain, the CRB2

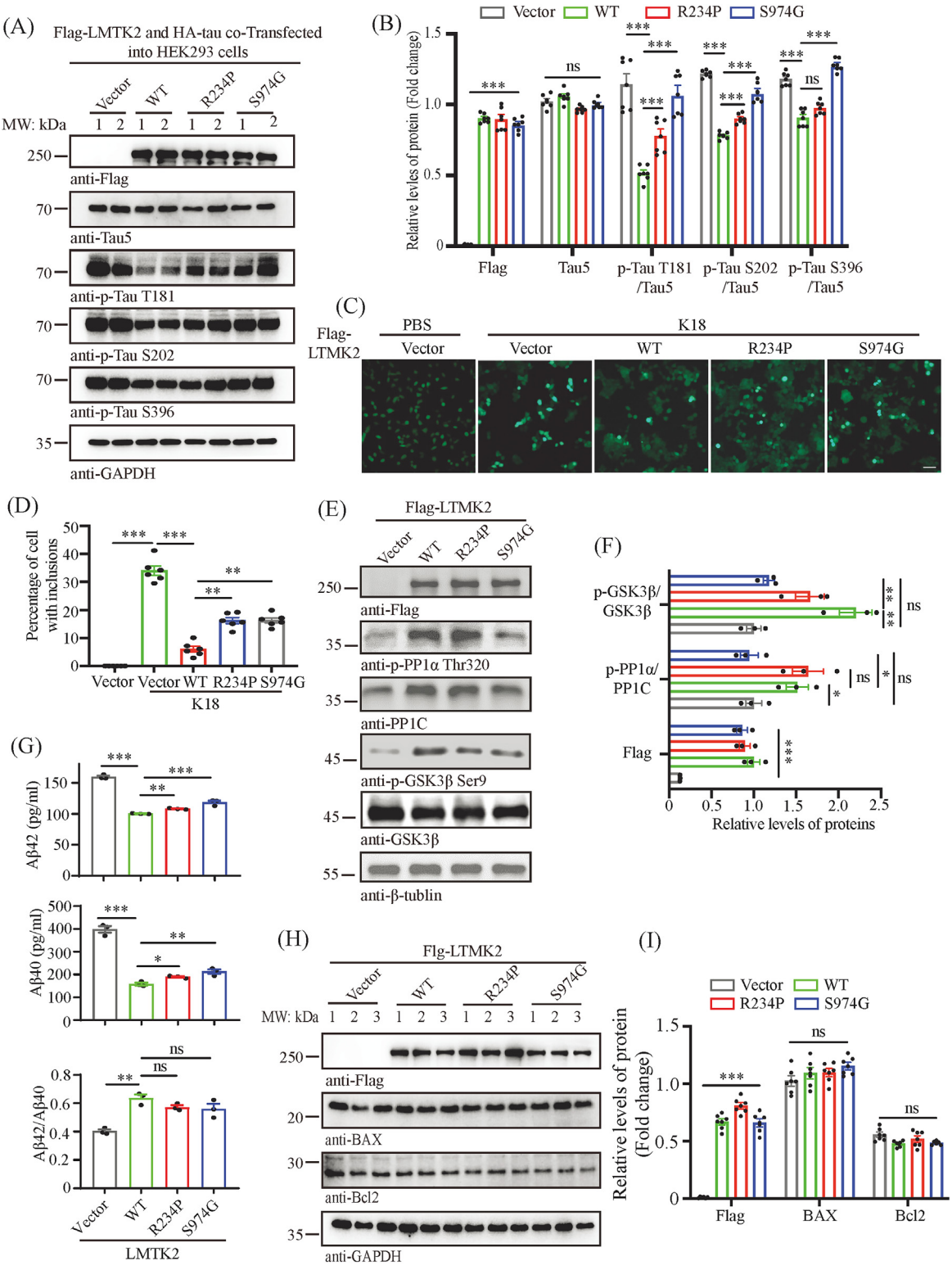

Fig. 3. Effects of the rare variants R234P or S974G of *LMTK2* on Tau aggregation, Aβ generation, and apoptosis *in vitro*. (A) Western blot analysis of phosphorylation levels of Tau and total Tau after Flag-LMTK2 and HA-Tau plasmids were co-transfected into HEK293 cells for 48 h. (B) Quantification of relative protein levels in A ($n = 6$). (C) Representative images of K18-induced Tau aggregation after HEK293-Tau RD cells were transfected with LMTK2. After LMTK2 plasmid transfection for 24 h, K18 (1μg/μL) was added, induced for 48 h, and photographed by a fluorescence microscope. Scale bar: 20 μm (D) Quantification of cell with inclusions in C ($n = 6$). (E) Western blot analysis of the effect of LMTK2 WT and variants on PP1C-GSK3β signaling pathway. (F) Quantification of relative protein levels in E ($n = 3$). (G) ELISA detection of secreted Aβ after LMTK2 WT and variants were transfected into SH-SHY5Y-APPSwe cells ($n = 3$). (H) Western blot analysis of BAX and Bcl2 expression after LMTK2 WT and variants were transfected into SH-SHY5Y-APPSwe cells. (I) Quantification of relative BAX and Bcl2 expression ($n = 6$). Western blot data are representative of three independent experiments. Data are mean ± SEM, *, * and *** represent $p < 0.05$, $p < 0.01$, and $p < 0.001$, respectively, and ns represents no statistical significance (Student's *t*-test).

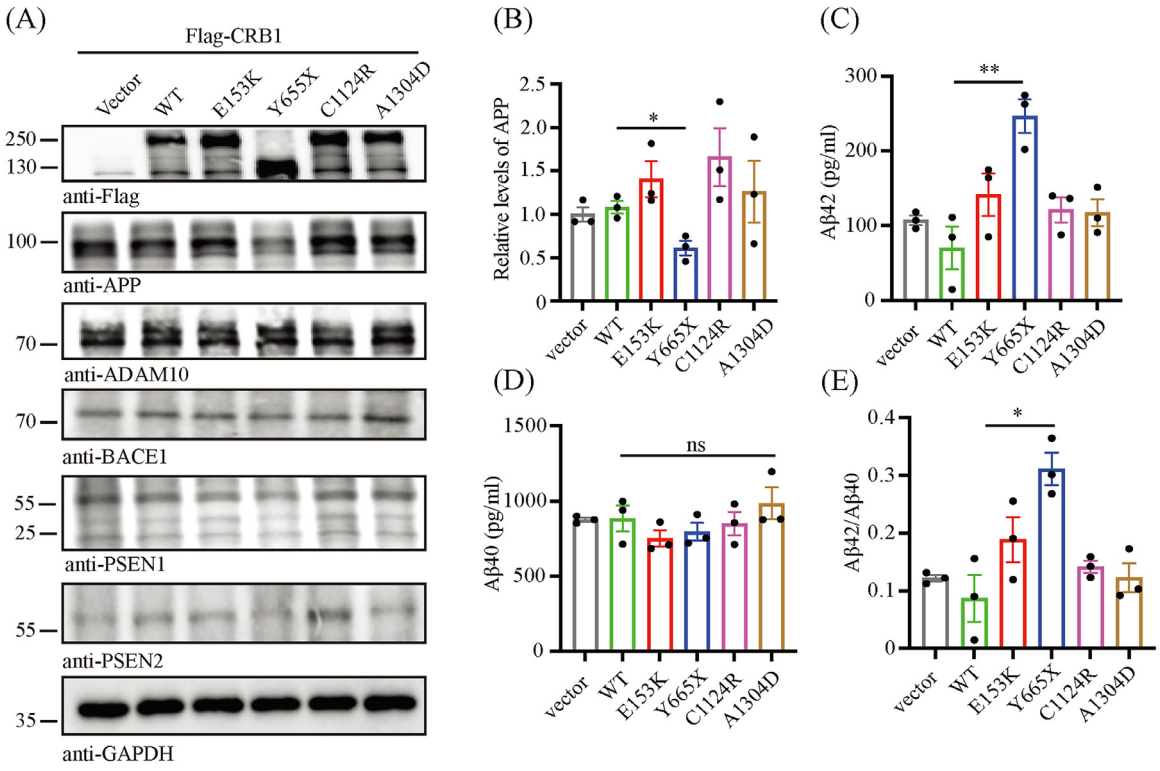

Fig. 4. Effect of rare variants in CRB1 on Aβ generation. (A) WB detection of APP and related secretory enzymes expression after high expression of different CRB1 plasmids in SH-SY5Y-APPSwe cells. (B) Quantification of related APP expression. (C-E) ELISA detection of the concentration of Aβ42 (C), Aβ40 (D), and the Aβ42/Aβ40 ratio (E) in the culture medium after the overexpression of different CRB1 plasmids in SH-SY5Y-APPSwe cells. Western blot data are representative of three independent experiments. Data are mean ± SEM, * and ** represent $p < 0.05$ and $p < 0.01$, respectively, and ns represents no statistical significance (Student's *t*-test).

level is significantly elevated, suggesting a potential compensating response to CRB1 dysfunction [50]. It is reported that *Drosophila* Crumbs protein reduces Notch signaling by inhibiting γ-secretase activity at the wing margins [51]. In HEK293 cells, the overexpression of CRB1 or additional Crumbs isoforms (CRB2, CRB3) did not affect the Aβ level [52]. Nonetheless, the overexpression of CRBs led to a substantial reduction of Aβ in HEK293/wtAPP cells and SH-SY5Y cells. This work contradicts the prior research, potentially due to the low levels of produced Aβ in HEK293 cells [53]. Since γ-secretase mediates Aβ generation, Crumbs protein is presumed to modulate Aβ metabolism. Interestingly, patients with *CRB1* retinopathy had superior memory and learning abilities compared to persons without CRB1 retinopathy and normal controls, potentially attributable to compensatory adaptations resulting from visual impairment [54]. In this study, The Y665X is a stop-gain variant, which leads to the expression of truncated CRB1 protein, which was confirmed in the WB result of anti-Flag (Fig. 4A). Although CRB1 WT and its three rare damaging missense variants (E153K, C1124R, and A1304D) did not significantly affect Aβ generation, the stop-gain variant (Y655X) did stimulate an increase in Aβ42, which indicates a crucial relationship between innate domains of CRB1 and its physiological function.

Meanwhile, our study has several limitations. All of the individuals were from Central Southern China. The environment and dietary habits are similar in this region. Since we mainly enrolled AD patients in Hunan province, the AD patients with *LMTK2* or *CRB1* rare variants were from Hunan. Consequently, the variants may be not associated with environmental factors. Although we conducted a replication study to verify the rare damaging variants in *LMTK2* and *CRB1* by analyzing the same AD patients and controls sequenced through WGS, future studies in larger cohorts of EOAD/FAD patients are necessary to confirm these associations in other cohorts. Regarding the mechanism of mutated *LMTK2* and *CRB1* on the pathogenesis of AD, it remains essential to examine their roles in animal models, especially for *CRB1* rare variants in this study. Future investigations to address these key issues may help better understand the roles of *LTMK2* and *CRB1* in the onset of AD.

In conclusion, we conducted WES in the Chinese population to successfully identify two novel risk genes for AD, utilizing an extreme phenotype sampling strategy with EOAD/FAD patients alongside controls. We initially observed that LMTK2 downregulates the levels of Aβ42 and Aβ40 and demonstrated that rare damaging variants of *LMTK2* impair its physiological functions and adversely affect tau phosphorylation and APP metabolism. Additionally, the damaging variant of *CRB1* led to incomplete translation of CRB1 protein and increased the Aβ level.

Fundings

This study was supported by the National Natural Science Foundation of China (U22A20300, 82371434, 82071216), STI2030-Major Projects (2021ZD0201803), National Key R&D Program of China (2023YFC3603700), Outstanding Youth Fund of Hunan Provincial Natural Science Foundation (2024JJ2097), Hunan Health Commission Grant (20232460), Science and Technology Major Project of Hunan Province (2021SK1020), Postdoctoral Fellowship Program of CPSF (GZC20233185), and The Scientific Research Program of FuRong Laboratory (2024PT5108).

Authorship contributions

Xuewen Xiao performed the analyses and wrote the manuscript. Shilin Luo and Hui Liu contributed to the functional examination. Xuewen Xiao, Rui Yao, Yunni Li, Xinxin Liao, Yingzi Liu, Yafang Zhou, and Junling Wang collected the enrolled individuals. Beisha Tang, Bin Jiao, Jinchen Li, Lu Shen, and Shilin Luo supervised the analyses. Shilin Luo coordinated the study and wrote the manuscript. All authors read and approved the final manuscript.

Ethics approval

The study was conducted in accordance with the Helsinki Declaration and was approved by the Ethics Committee of Xiangya Hospital, Central South University, China.

Declaration of interests

The authors declare the following financial interests/personal relationships which may be considered as potential competing interests:

Shilin Luo reports financial support was provided by National Natural Science Foundation of China. If there are other authors, they declare that they have no known competing financial interests or personal relationships that could have appeared to influence the work reported in this paper.

CRediT authorship contribution statement

Xuewen Xiao: Writing – review & editing, Writing – original draft, Visualization, Validation, Project administration, Methodology, Investigation, Formal analysis, Data curation. **Hui Liu:** Methodology, Investigation, Formal analysis, Conceptualization. **Rui Yao:** Formal analysis, Data curation. **Yunni Li:** Data curation. **Xinxin Liao:** Data curation. **Yingzi Liu:** Data curation. **Yafang Zhou:** Data curation. **Junling Wang:** Data curation, Conceptualization. **Beisha Tang:** Data curation, Conceptualization. **Bin Jiao:** Supervision, Resources, Project administration, Methodology, Investigation, Data curation, Conceptualization. **Jinchen Li:** Validation, Supervision, Resources, Project administration, Methodology, Investigation, Formal analysis, Data curation, Conceptualization. **Lu Shen:** Visualization, Validation, Supervision, Resources, Project administration, Methodology, Investigation, Funding acquisition, Formal analysis, Data curation, Conceptualization. **Shilin Luo:** Writing – review & editing, Visualization, Validation, Supervision, Resources, Project administration, Methodology, Investigation, Funding acquisition, Formal analysis, Data curation, Conceptualization.

Supplementary materials

Supplementary material associated with this article can be found, in the online version, at doi:10.1016/j.tjpad.2025.100087.

References

[1] Scheltens P, De Strooper B, Kivipelto M, et al. Alzheimer's disease. Lancet 2021;397(10284):1577–90.
[2] Jack CR Jr, Andrews JS, Beach TG, et al. Revised criteria for diagnosis and staging of Alzheimer's disease: Alzheimer's Association Workgroup. Alzheimer Dement 2024;20(8):5143–69.
[3] Sims R, Hill M, Williams J. The multiplex model of the genetics of Alzheimer's disease. Nat Neurosci 2020;23(3):311–22.
[4] Goate A, Chartier-Harlin M-C, Mullan M, et al. Segregation of a missense mutation in the amyloid precursor protein gene with familial Alzheimer's disease. Nature 1991;349(6311):704–6.
[5] Sherrington R, Rogaev E, Ya Liang, et al. Cloning of a gene bearing missense mutations in early-onset familial Alzheimer's disease. Nature 1995;375(6534):754–60.
[6] Levy-Lahad E, Wasco W, Poorkaj P, et al. Candidate gene for the chromosome 1 familial Alzheimer's disease locus. Science 1995;269(5226):973–7.
[7] Jiao B, Liu H, Guo L, et al. The role of genetics in neurodegenerative dementia: a large cohort study in South China. NPJ Genom Med 2021;6(1):69.
[8] Nudelman KN, Jackson T, Rumbaugh M, et al. Pathogenic variants in the Longitudinal Early-onset Alzheimer's Disease Study cohort. Alzheimer Dement 2023;19:S64–73.
[9] Andrews SJ, Renton AE, Fulton-Howard B, Podlesny-Drabiniok A, Marcora E, Goate AM. The complex genetic architecture of Alzheimer's disease: novel insights and future directions. EBioMedicine 2023:90.
[10] Wetzel-Smith MK, Hunkapiller J, Bhangale TR, et al. A rare mutation in UNC5C predisposes to late-onset Alzheimer's disease and increases neuronal cell death. Nat Med 2014;20(12):1452–7.
[11] Jonsson T, Stefansson H, Steinberg S, et al. Variant of TREM2 associated with the risk of Alzheimer's disease. N Engl J Med 2013;368(2):107–16.
[12] Cruchaga C, Karch CM, Jin SC, et al. Rare coding variants in the phospholipase D3 gene confer risk for Alzheimer's disease. Nature 2014;505(7484):550–4.
[13] Belloy ME, Andrews SJ, Le Guen Y, et al. APOE genotype and Alzheimer disease risk across age, sex, and population ancestry. JAMA Neurol 2023;80(12):1284–94.
[14] Jia L, Du Y, Chu L, et al. Prevalence, risk factors, and management of dementia and mild cognitive impairment in adults aged 60 years or older in China: a cross-sectional study. Lancet Public Health 2020;5(12):e661–ee71.
[15] Zhang D-F, Fan Y, Xu M, et al. Complement C7 is a novel risk gene for Alzheimer's disease in Han Chinese. Natl Sci Rev 2019;6(2):257–74.
[16] McKhann GM, Knopman DS, Chertkow H, et al. The diagnosis of dementia due to Alzheimer's disease: recommendations from the National Institute on Aging-Alzheimer's Association workgroups on diagnostic guidelines for Alzheimer's disease. Alzheimer Dement 2011;7(3):263–9.
[17] Li H, Durbin R. Fast and accurate long-read alignment with Burrows-Wheeler transform. Bioinformatics 2010;26(5):589–95.
[18] McKenna A, Hanna M, Banks E, et al. The genome analysis toolkit: a mapreduce framework for analyzing next-generation DNA sequencing data. Genom Res 2010;20(9):1297–303.
[19] Wang K, Li M, Hakonarson H. ANNOVAR: functional annotation of genetic variants from high-throughput sequencing data. Nucl Acid Res 2010;38(16) e164-e.
[20] Li J, Zhao T, Zhang Y, et al. Performance evaluation of pathogenicity-computation methods for missense variants. Nucl Acid Res 2018;46(15):7793–804.
[21] Huang Y, Bodnar D, Chen C-Y, et al. Rare genetic variants impact muscle strength. Nat Commun 2023;14(1):3449.
[22] Den Dunnen JT, Dalgleish R, Maglott DR, et al. HGVS recommendations for the description of sequence variants: 2016 update. Hum Mutat 2016;37(6):564–9.
[23] Chang CC, Chow CC, Tellier LC, Vattikuti S, Purcell SM, Lee JJ. Second-generation PLINK: rising to the challenge of larger and richer datasets. Gigascience 2015;4(1) s13742-015-0047-8.
[24] Meng L, Liu C, Liu M, et al. The yeast protein Ure2p triggers Tau pathology in a mouse model of tauopathy. Cell Rep 2023;42(11).
[25] Lee S, Emond MJ, Bamshad MJ, et al. Optimal unified approach for rare-variant association testing with application to small-sample case-control whole-exome sequencing studies. Am J Hum Genet 2012;91(2):224–37.
[26] Chia R, Ray A, Shah Z, et al. Genome sequence analyses identify novel risk loci for multiple system atrophy. Neuron 2024.
[27] Sanders DW, Kaufman SK, DeVos SL, et al. Distinct tau prion strains propagate in cells and mice and define different tauopathies. Neuron 2014;82(6):1271–88.
[28] Bencze J, Mórotz GM, Seo W, et al. Biological function of Lemur tyrosine kinase 2 (LMTK2): implications in neurodegeneration. Mol Brain 2018;11:1–9.
[29] Mitsuishi Y, Hasegawa H, Matsuo A, et al. Human CRB2 inhibits gamma-secretase cleavage of amyloid precursor protein by binding to the presenilin complex. J Biol Chem 2010;285(20):14920–31.
[30] Reitz C, Pericak-Vance MA, Foroud T, Mayeux R. A global view of the genetic basis of Alzheimer disease. Nat Rev Neurol 2023;19(5):261–77.
[31] Cruz DF, Farinha CM, Swiatecka-Urban A. Unraveling the function of lemur tyrosine kinase 2 network. Front Pharmacol 2019;10:24.
[32] Kesavapany S, Lau K-F, Ackerley S, et al. Identification of a novel, membrane-associated neuronal kinase, cyclin-dependent kinase 5/p35-regulated kinase. J Neurosci 2003;23(12):4975–83.
[33] Bencze J, Szarka M, Bencs V, et al. Neuropathological characterization of Lemur tyrosine kinase 2 (LMTK2) in Alzheimer's disease and neocortical Lewy body disease. Sci Rep 2019;9(1):17222.
[34] Mórotz GM, Glennon EB, Gomez-Suaga P, et al. LMTK2 binds to kinesin light chains to mediate anterograde axonal transport of cdk5/p35 and LMTK2 levels are reduced in Alzheimer's disease brains. Acta Neuropathol Commun 2019;7:1–16.
[35] Zhang L, Shu F. LMTK2 inhibits Ab25-35-elicited ferroptosis, oxidative stress and apoptotic damage in PC12 cells through activating Nrf2/ARE signalling pathway. Folia neuropathol 2023;62(1):47–58.
[36] Duyckaerts C, Delatour B, Potier M-C. Classification and basic pathology of Alzheimer disease. Acta Neuropathol 2009;118:5–36.
[37] Manser C, Guillot F, Vagnoni A, et al. Lemur tyrosine kinase-2 signalling regulates kinesin-1 light chain-2 phosphorylation and binding of Smad2 cargo. Oncogene 2012;31(22):2773–82.
[38] Manser C, Vagnoni A, Guillot F, Davies J, Miller CC. Cdk5/p35 phosphorylates lemur tyrosine kinase-2 to regulate protein phosphatase-1C phosphorylation and activity. J Neurochem 2012;121(3):343–8.
[39] Bencze J, Szarka M, Bencs V, Szabó RN, Módis LV, Aarsland D, et al. Lemur tyrosine kinase 2 (LMTK2) level inversely correlates with phospho-tau in neuropathological stages of Alzheimer's disease. Brain Sci 2020;10(2):68.
[40] Matarin M, Salih DA, Yasvoina M, et al. A genome-wide gene-expression analysis and database in transgenic mice during development of amyloid or tau pathology. Cell Rep 2015;10(4):633–44.
[41] Karran E, De Strooper B. The amyloid hypothesis in Alzheimer disease: new insights from new therapeutics. Nat Rev Drug Discov 2022;21(4):306–18.
[42] Lauretti E, Dincer O, Praticò D. Glycogen synthase kinase-3 signaling in Alzheimer's disease. Biochim Biophys Acta Mol Cell Res 2020;1867(5):118664.
[43] Miyagawa T, Ebinuma I, Morohashi Y, et al. BIN1 regulates BACE1 intracellular trafficking and amyloid-β production. Hum Mol Genet 2016;25(14):2948–58.
[44] Thomas S, Hoxha K, Tran A, Prendergast GC. Bin1 antibody lowers the expression of phosphorylated Tau in Alzheimer's disease. J Cell Biochem 2019;120(10):18320–31.
[45] Ando K, Nagaraj S, Küçükali F, et al. PICALM and Alzheimer's disease: an update and perspectives. Cells 2022;11(24):3994.
[46] Alves CH, Pellissier LP, Wijnholds J. The CRB1 and adherens junction complex proteins in retinal development and maintenance. Prog Retin Eye Res 2014;40:35–52.
[47] Varela MD, Georgiou M, Alswaiti Y, et al. CRB1-associated retinal dystrophies: genetics, clinical characteristics, and natural history. Am J Ophthalmol 2023;246:107–21.

[48] den Hollander AI, Ghiani M, de Kok YJ, et al. Isolation of Crb1, a mouse homologue of Drosophila crumbs, and analysis of its expression pattern in eye and brain. Mech Dev 2002;110(1–2):203–7.
[49] Atlas HP. A human protein atlas for normal and cancer tissues. PNAS 2008;104(49):19428–33.
[50] Dolón JF, Paniagua AE, Valle V, et al. Expression and localization of the polarity protein CRB2 in adult mouse brain: a comparison with the CRB1rd8 mutant mouse model. Sci Rep 2018;8(1):11652.
[51] Herranz H, Stamataki E, Feiguin F, Milán M. Self-refinement of notch activity through the transmembrane protein crumbs: modulation of γ-secretase activity. EMBO Rep 2006;7(3):297–302.
[52] Pardossi-Piquard R, Chen F, et al. Overexpression of human CRB1 or related isoforms, CRB2 and CRB3, does not regulate the human presenilin complex in culture cells. Biochemistry 2007;46(48):13704–10.
[53] Mitsuishi Y, Hasegawa H, Matsuo A, et al. Human CRB2 inhibits γ-secretase cleavage of amyloid precursor protein by binding to the presenilin complex. J Biol Chem 2010;285(20):14920–31.
[54] Wright GA, Rodriguez-Martinez AC, Conn H, Matarin M, Thompson P, Moore AT, et al. Enhanced learning and memory in patients with CRB1 retinopathy. Genes (Basel) 2024;15(6):660.